Optimization of Visible Light Positioning in Industrial Applications using Machine Learning

Youniss Alkandari, Muhammad Ijaz,
Sunday Ekpo, Bamidele Adebisi
School of Engineering
Manchester Metropolitan University
Manchester, United Kingdom
Youniss.Alkandari, m.ijaz, @stu.mmu.ac.uk

Ismael Soto, Raul Zamorano-Illanes
Department of Electrical Engineering
Santiago de Chile University
Santiago, Chile
{ismael.soto, raul.zamorano}, @usach.cl

Cesar Azurdia
Department of Electrical Engineering
Universidad de Chile
Santiago, Chile
cesarazurdia@uchile.cl

Abstract—This paper investigates the error performance of visible Light Positioning (VLP) systems for 3D indoor drone localization using machine learning algorithms. Received Signal Strength is used to track the position of the drone and different smoky channel conditions to emulate an industrial environment. VLP systems utilize visible light communication (VLC) and indoor positioning, providing a low-cost and interference-free solution for precise drone localization. Machine learning (ML) based artificial neural network (ANN) is used to trained on diverse datasets and correlations between received signal strength (RSS) measurements and position errors. The results demonstrate that ML enables accurate real-time drone position estimation, compensating for atmospheric attenuation. The trained models achieve significantly improved localization accuracy and capturing non-linear relationships between input features and drone location. Furthermore, machine learning algorithms extract relevant features, reducing the impact of noise and atmospheric attenuations. ML process enhances the VLP system's robustness, resulting in remarkable localization accuracy improvements compared to the attenuated path with average error values from 21.9 cm to 5.9 cm. The trained ML models achieve RMSE values of 0.044772 and 0.067523, respectively, with high R-squared values of 0.999. Furthermore the error histogram analysis confirms accurate drone location estimation, even in the presence of atmospheric attenuations.

Index Terms—Indoor Localization, Industrial Environment, Visible Light Positioning, Atmospheric Attenuation, Machine Learning.

I. INTRODUCTION

Unmanned Aerial Vehicles (UAVs), also known as drones, have emerged as versatile devices for use in indoor industrial applications, providing automated autonomous operations in industrial applications and cost-effective solutions for managing supplies [1]. Their potential applications include automobile industry, food industry, power plants, warehouses, and smart farming, where they perform duties such as facade inspections and animal feed distribution. Additionally, drones are used to investigate nuclear sites and detect damages or leaks within structures [2].

VLP systems are utilized in conjunction with machine learning techniques to facilitate accurate localization of drones in indoor environments. VLP makes use of VLC and indoor positioning systems, employing LED-based infrastructure typically found in buildings and industrial sites [3], [4],

allowing 3D positioning in difficult environments, such as underground mining, within a large number of particles and complex channel effects [5]. This method provides a low-cost and interference-free solution for the precise localization and tracking of drones using a LED arrangement on a Lattice architecture [6]. VLP provides superior accuracy and operates without electromagnetic interference, making it an optimal choice for indoor drone positioning, according to research [7].

However, due to atmospheric conditions, reliable and precise drone localization in indoor environments is difficult to achieve. Traditional VLP systems presume clear air as the gearbox medium, but in industrial settings, smoke, fog, and other particles may be present in varying concentrations. These atmospheric conditions such as dust, smog, smoke and water particles such as fog could attenuate the received signal strength (RSS) at the drone's receivers [7], [8]. Significant progress has been made over the past decade in the development and performance enhancement of VLP systems [9]. Existing systems concentrate primarily on two-dimensional (2D) positioning in clear air, leaving a critical gap in addressing the influence of atmospheric attenuations on received power and VLP accuracy for UAV flight paths [7].

In bridging this disparity, machine learning plays a crucial role in improving VLP systems. These systems can overcome the challenges posed by atmospheric conditions and enhance their performance by utilizing machine learning techniques. The training of machine learning algorithms on large datasets that include various atmospheric conditions enables the models to discover patterns and correlations between RSS measurements and drone coordinates in specific environments [10], [11].

These trained machine learning models enable estimation of the drone's position in real time, compensating for signal degradation due to smoke, smog, or other atmospheric attenuation. By analyzing the received power and pertinent sensor data, the models accurately predict the location of the drone, allowing for reliable indoor positioning even in challenging atmospheric conditions. Moreover, ML techniques allow for the continuous optimization's of VLP systems by refining algorithms through iterative learning and adaptation, thereby enhancing accuracy and robustness in dynamic environments
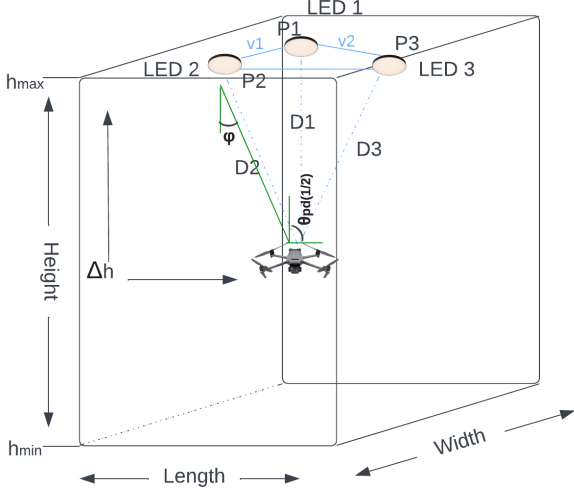
Fig. 1. The overview of the room's cross-section and the schematic diagram for the trilateration problem and its parameters.

[12].

This paper investigate the role of machine learning in improving VLP for indoor drone localization in light of these advancements. Specifically, it addresses the impact of atmospheric attenuations on received power and VLP accuracy for UAV flight paths, thereby filling a critical void in the existing research. This research seeks to develop a more dependable and accurate VLP system capable of overcoming the obstacles posed by industrial atmospheric conditions by leveraging machine learning algorithms and large datasets.

II. SYSTEM MODEL

Figure 1 shows the schematic of the considered system. It consists of a typical industrial environment (25m × 15m × 5m) with 15 uniformly distributed light fixtures on the ceiling with 1 LED per light fixture with 5m spacing per transmitter. Each light fixture has a half semi-angle of 60° and a power of 80 Watts, strong output luminaires being typical in industrial environments [13]. The main simulation parameters are shown in Table 1.

The N light fixtures are placed at a fixed height hLED with coordinates $(x_i, y_i, h_{LED}) i = 1 \cdots N$. The receiver, with a photodetector (PD) area A_{pd} is located at the unknown location (x, y, z). For typical LEDs with Lambertian radiation pattern m, the received power P_{ri} from ith transmitter is given by [14].

$$P_{ri} = \begin{cases} P_{ti} \frac{(m+1)A_{pd}}{2\pi d_i^2} cos^m(\phi)cos(\varphi)H_{Att} & , \quad \varphi \leq \theta_{pd} \\ 0 & , \quad \varphi > \theta_{pd} \end{cases} \quad (1)$$

where P_{ti} is the transmitter power, d_i is the distance between the transmitter and the receiver, ϕ is the angle of irradiance, φ is the angle of incidence, and θ_{pd} is the field

of view of the receiver, as shown in Figure 1. The effect of indoor attenuation is described with the help of the attenuation coefficient H_{Att} in respect to the propagation length L and is described as the following:

$$H_{Att} = e^{-\beta_\lambda L} \quad (2)$$

The effect of smoke and fog attenuation has been considered in (1) and (2) using the laboratory-based smoke and fog model and the proposed q values, which are the particle size distribution coefficient for both models are shown in [15] and is given by:

$$\beta(dB/km) = \frac{17}{V(km)} \left(\frac{\lambda}{\lambda_0} \right)^{-q(\lambda)} \quad (3)$$

$$q(\lambda) = \begin{cases} 0.1428\lambda - 0.0947 & Fog \\ 0.8467\lambda - 0.5212 & Smoke \end{cases} \quad (4)$$

The distance between the transmitter and the receiver d_i can be calculated from the received signal power, P_{ri}. Moreover, given $cos(\phi) = cos(\varphi) = \frac{h_{LED} - z}{d_i} = \frac{\Delta h}{d_i}$ for horizontally oriented transmitters and receiver, the estimated distance $\hat{d}_i$ can be calculated as [15]:

$$\hat{d}_i = \sqrt[m+3]{\frac{(m+1)A_{pd}P_t\Delta h^{m+1}}{2\pi P_{ri}}} \quad (5)$$

where $\Delta h = h_{LED} - z$ is the vertical height difference between the transmitter and the receiver, therefore, h is varied. Note that, the estimated distance d_i cannot be directly calculated from without knowing the accurate Δh. Due to this, we generate a set of estimated distances $\hat{d}_i$ for different possible heights h should be z ranging from $0m$ $(h_m in)$ to h_{LED} with height resolution R_h of $1mm$. This leads to the accurate estimation of $\hat{d}_i$. The received signal is affected by shot and thermal noises with the total variance $\sigma_{shot}^2 + \sigma_{therma}^2$. The signal-to-noise ($SNR$) ratio can be calculated using:

$$SNR_i(dB) = 10log \frac{(R_r P_{ri})^2}{\sigma_{noise}^2} \quad (6)$$

where, R_r is the receiver's PD responsivity.

A. Positioning Algorithm

Then, the positioning algorithm is performed for each of the sets of generated distances $\hat{d}_i (i = 1 \cdots N)$ at different heights using (5). Figure 1 shows the three transmitters $p1$, $p2$, and $p3$ positions and with $p4$ being the unknown drone location. The algorithm only requires three transmitter positions, meaning that the corresponding signals from the three nearest (i.e. strongest) LEDs are taken into account, as they offer the highest SNR.

The Cayley-Menger bideterminant of two sequences of n points $[p_1, p_2, \cdots, p_n]$ and $[q_1, q_2, \cdot, q_n]$ is defined as [16]:

$$D(p_1, \cdots, p_n; q_1, \cdots, q_n) = 2\left(\frac{-1}{2}\right)^n \begin{vmatrix} 0 & 1 & 1 & 1 & 1 \\ 1 & D(p_1, q_1) & D(p_1, q_2) & \cdots & D(p_1, q_n) \\ 1 & D(p_2, q_1) & D(p_2, q_2) & \cdots & D(p_1, q_n) \\ 1 & \vdots & \vdots & \ddots & \vdots \\ 1 & D(p_n, q_1) & D(p_n, q_2) & \cdots & D(p_n, q_n) \end{vmatrix} \quad (7)$$

Parameter	Value
Width × Length × Height	25 m × 15 m × 5 m
Transmitter's Electrical Power - Pt_t	80 W
Transmitter's semi-angle ϕ	60°
Receiver's Height	0.1 – 3.6 m
Photodetector Area - A_{pd}	1 cm^2
Receiver's FOV (half-angle) - $\theta_{pd(1/2)}$	80°
Receiver's Responsivity - R_r	0.54 A/W
Bandwidth	10 MHz
Visibility for fog and smoke	0.3 km - 1 km
Optical Filter	450 nm
Trained data size	478 MB
Number of hidden layers	100 layers
Number of epochs	1000

where $D(p_i; q_j)$ is the squared distance between points p_i and p_j. When two sequences of points are the same, then $D(p_1, \cdots, p_n; q_1, \cdots, q_n)$ is denoted by $D(p_1, \cdots, p_n)$ and CMD is given by:

$$D(p_1, p_2, p_3, p_4) = \frac{1}{8} \begin{vmatrix} 0 & 1 & 1 & 1 & 1 \\ 1 & 0 & D(p_1, p_2) & D(p_1, p_3) & D(p_1, p_4) \\ 1 & D(p_2, p_1) & 0 & D(p_2, p_3) & D(p_2, p_4) \\ 1 & D(p_3, p_1) & D(p_3, p_2) & 0 & D(p_3, p_4) \\ 1 & D(p_4, p_1) & D(p_4, p_2) & D(p_4, p_3) & 0 \end{vmatrix}, \quad (8)$$

where p4 is the location of the drone, meaning that $D(p_4, p_1), D(p_4, p_2), D(p_4, p_3)$ are distances $\hat{d}_1, \hat{d}_2, \hat{d}_3$ that are computed from the received power measurements. It is possible to calculate the position of the receiver p_4 with respect to three known transmitter coordinates (p_1, p_2, p_3) using:

$$p_4 = p_1 + k_1 v_1 + k_2 v_2 \pm k_3(v_1 v_2) \quad (9)$$

where $v_1 = p_2 + p_1$, $v_2 = p_3 - p_1$,

$$k_1 = -\frac{D(p_1, p_2, p_3; p_1, p_3, p_4)}{D(p_1, p_2, p_3)},$$

$$k_2 = \frac{D(p_1, p_2, p_3; p_1, p_3, p_4)}{D(p_1, p_2, p_3)},$$

$$k_3 = \frac{sqrt(D(p_1, p_2, p_3, p_4))}{D(p_1, p_2, p_3)}$$

This results in a single estimate $p_4 = (\hat{x}, \hat{y}, \hat{z})$ for each of the heights.

Once all possible locations have been generated, the estimated location is found at the minimum of $C(h)$, with $C(h)$ being the average squared error between the estimated distances $\hat{d}_1$ calculated using (5), and the distances of the estimated location $(\hat{x}, \hat{y}, \hat{z})$ from (9). The cost function finds the minima at the receiver's actual height, given by [17]

$$C(h) = \frac{1}{N} \sum_{i=1}^{N} \left[\hat{d}_i - \sqrt{(\hat{x} - x_i)^2 + (\hat{y} - y_i)^2 + (\hat{z} - z_i)^2} \right]^2 \quad (10)$$

where $z_i = h_L ED$.

Using the presented algorithm, the (x, y, z) coordinates of the receiver can be estimated. After calculating the position, the estimated position is compared with the actual position to find the positioning error, given by:

$$D_{error} = \sqrt{(\hat{x} - x)^2 + (\hat{y} - y)^2 + (\hat{z} - z)^2} \quad (11)$$

B. Machine Learning Model

To enhance the localization accuracy on the 3D position estimation of the drone, ML algorithms, specifically neural networks (ANN) are employed. These models capture complex relationships between the input features obtained from the positioning algorithm, taking as reference the desired trajectory point of the drone, one axis at a time, allowing for improved the positioning applying three different models [18].

ANN is chosen as the ML algorithm for visible light positioning in the industrial environment because of its ability to handle complex and non-linear relationships between input features and the desired output. Compared to other ML techniques, ANN excel in capturing intricate patterns and representations from the dataset. To improve the accuracy of the training, a dataset of trajectories of drone is generated by applying the positioning algorithm as shown in Fig.2. This allows to train the ML model within enough information. The simulation environment incorporates smoke and fog attenuations to replicate real-world conditions where visibility is impaired.
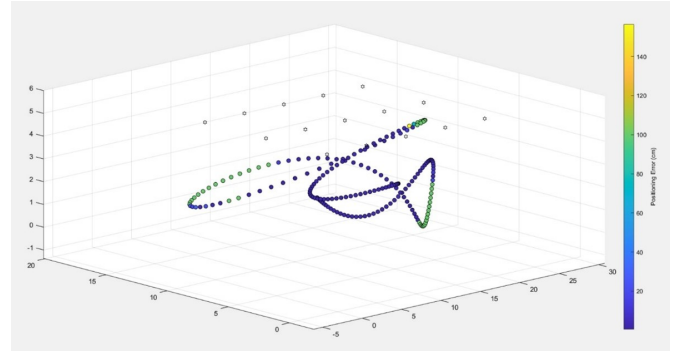

Fig. 2. Simulated drone trajectory on a 7x7 meters sized room with a 15 visible light emitters arrangement measuring the positioning error of original the algorithm.

By subjecting the drone to these simulated environmental factors, the model can learn to predict the drone's location more accurately, even in challenging scenarios [18].

The training data includes several parameters, firstly the real 3D position in X, Y, and Z coordinates. The presence of smoke and fog introduce error on the algorithm estimation, which is measured on each point, resulting in attenuated or distorted trajectories. The position values of X, Y and Z axis derived from the simulated data represent these attenuated locations.

Using this dataset, the ANN is trained to map the attenuated locations to the true locations of the drone. The network learns to identify patterns and features within the data that can help it make accurate predictions. Through an iterative learning process, the ANN adjusts its internal parameters to minimize

the error between the predicted and true locations, enhancing the drone's localization accuracy. In order to reduce the error, the network architecture must be evaluated, specifying the density of its layers and the depth of the model, to later in the training carry out an analysis of the error in relation to the epochs, finding the optimal point [19].

Overall, ANN provide a powerful framework for addressing the challenges of drone localization in an industrial environment with smoke and fog attenuations. Their non-linear nature, feature extraction capabilities, and adaptability contribute to reducing the error percentage and improving the accuracy of the drone's location estimation.

III. RESULTS AND DISSCUSSION

In this section, simulation results are presented in terms of trained model performance, trained model path compared with the real path and the attenuated path.

Figure 3 shows the best validation performance of the trained model when compared to the mean squared error (MSE) and the number of epochs. Specifically, the model achieves an impressively low MSE value of 0.0001825 at the 1000 epoch, demonstrating its capability to effectively minimize the difference between predicted and actual values. Furthermore, the root mean squared error (RMSE) of the model is reported to be 0.0431, indicating the average magnitude of the residuals.

Moreover, a notable aspect of the trained model is the consistent and smooth decrease observed in the trained, validated, and tested data. This behavior is indicative of the model's robustness and reliability, as it effectively handles the training, validation, and testing datasets without exhibiting any signs of instability or degradation. The coherence in the decreasing trends across these datasets further emphasizes the model's ability to generalize well and accurately predict the drone's localization, ultimately enhancing its overall performance.

Figure 4 describe the error histogram on the same three steps of the process, showing that the distribution follows the same trend, finding most values close to mean value of zero. The models trained to predict the values of the x and y axes obtained similar error values. The prediction of the positioning error along the x-axis "R_x_total" presented an RMSE of 0.044772, an R2 of 0.99999, a MSE of 0.0020045, and a MAE of 0.030362 were obtained. In the case of position error estimation using ML along y-axis "R_y_total" an RMSE of 0.067523, an R2 of 0.99989, a MSE of 0.0045593, and a MAE of 0.053228 are obtained. However, it is crucial to acknowledge that under conditions of attenuation, the estimated path of the drone does not precisely correspond with the real flight path, as evidenced in the inset of Figure 4. This discrepancy arises due to the reduction in RSS and SNR caused by the presence of smoke and fog attenuation, spanning a range of 0.3 km to 1 km. These attenuating factors introduce distortions in the received signals, impacting the model's ability to precisely estimate the drone's path.

Figure 5 shows the real flight trajectory, derived from a comprehensive dataset of 5 million positioning samples rang-

ing in height from 0.1 to 5 meters in the industrial warehouse, see Table 1 for detailed parameters. The results shows that the estimated flight path generated by the trained model using ANN closely aligns with the actual flight trajectory, exhibiting a high degree of accuracy.

Furthermore, Figure 5 inset presents the zoomed-in views of the trained, real, and attenuated paths. Notably, the trained path demonstrates a significantly closer alignment with the real path, boasting an average error rate of 5.9183. In contrast, the attenuated path appears considerably scattered away from the real path, displaying a notably higher average error rate of 21.9920. These observations underscore the remarkable improvement in localization accuracy achieved by the trained model while also highlighting the adverse impact of attenuation on localization accuracy in comparison. The results reaffirm that the trained model significantly enhances the drone's localization accuracy, effectively navigating within the industrial environment even amidst challenges posed by attenuation.
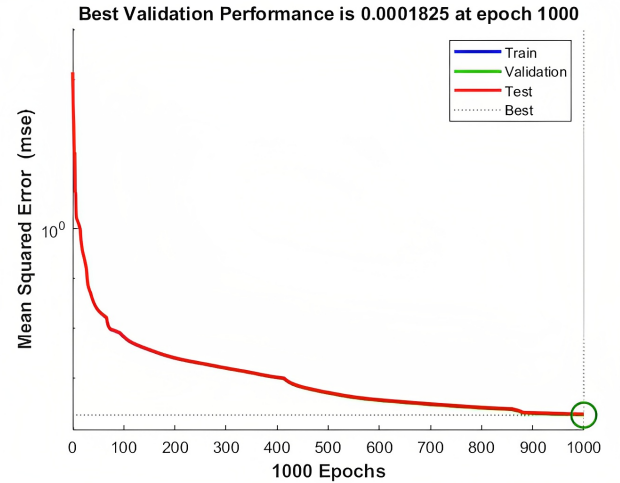

Fig. 3. Best validation performance of the trained model.

Figure 6 shows the trained path and the actual path of the drone. The difference between these two paths is an average of 0.1 cm upon closer inspection. This substantial reduction in the positioning error, when compared to the results obtained from the attenuated path, exemplifies the considerable improvement attained via the trained model. The reduced difference between the trained path and the actual path demonstrates the model's improved precision in estimating the drone's location in an industrial environment.

IV. CONCLUSION

This paper presents the implementation and investigation of ANN based ML algorithm to estimate the accuracy of 3D VLP in an industrial environment in the presence of harsh industry channel. The combination of VLP and machine learning techniques enables accurate real-time estimation of the drone's position, compensating for signal degradation caused by smoke, smog, or other atmospheric attenuation.
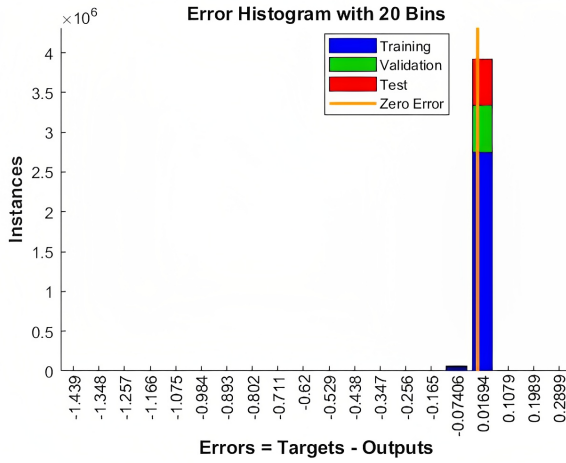
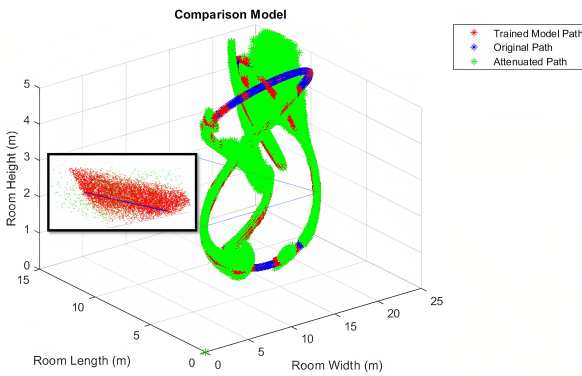Fig. 4. Error Histogram over the training, validation and test stages.

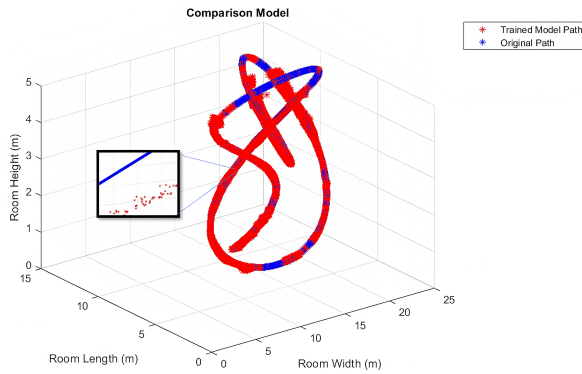Fig. 5. Selected real flight path and comparison with trained model and attenuated path.

Fig. 6. Selected real flight path and comparison with trained model.

The trained machine learning models achieved remarkable localization accuracy improvements, with an average error rate of 5.9183 for the trained path compared to 21.9920 for the attenuated path.

Moreover, the Error histogram analysis demonstrated that the trained models consistently estimated the drone's location accurately, even in the presence of atmospheric attenuations. Additionally, the machine learning models trained for "R_x_total" and "R_y_total" achieved high accuracy, with RMSE values of 0.044772 and 0.067523, respectively, and R-Squared values of 0.99999 and 0.99989, indicating the models' ability to capture intricate relationships between input features and the drone's location.

The results demonstrates the effectiveness of ML algorithms in automatically extracting relevant features from the data, reducing the impact of noise and atmospheric attenuations. The iterative learning process further enhanced the robustness of the VLP system, ensuring reliable and precise drone localization in dynamic industrial environments.

V. Acknowledgment

References

[1] T. Alladi, Naren, G. Bansal, V. Chamola, and M. Guizani, "Secauthuav: A novel authentication scheme for uav-ground station and uav-uav communication," *IEEE Transactions on Vehicular Technology*, vol. 69, no. 12, pp. 15 068–15 077, 2020.

[2] Y. Almadani, M. Ijaz, B. Adebisi, S. Rajbhandari, S. Bastiaens, W. Joseph, and D. Plets, "An experimental evaluation of a 3d visible light positioning system in an industrial environment with receiver tilt and multipath reflections," *Optics Communications*, vol. 483, p. 126654, 2021. [Online]. Available: https://www.sciencedirect.com/science/article/pii/S0030401820310725

[3] K. J. Wu, T. S. Gregory, J. Moore, B. Hooper, D. Lewis, and Z. T. H. Tse, "Development of an indoor guidance system for unmanned aerial vehicles with power industry applications," *IET Radar, Sonar and Navigation*, vol. 11, no. 1, pp. 212–218, 2017. [Online]. Available: https://ietresearch.onlinelibrary.wiley.com/doi/abs/10.1049/iet-rsn.2016.0232

[4] R. Liu, Z. Liang, K. Yang, and W. Li, "Machine learning based visible light indoor positioning with single-led and single rotatable photo detector," *IEEE Photonics Journal*, vol. 14, no. 3, pp. 1–11, 2022.

[5] A. Dehghan Firoozabadi, C. Azurdia-Meza, I. Soto, F. Seguel, N. Krommenacker, D. Iturralde, P. Charpentier, and D. Zabala-Blanco, "A novel frequency domain visible light communication (vlc) three-dimensional trilateration system for localization in underground mining," *Applied Sciences*, vol. 9, no. 7, 2019. [Online]. Available: https://www.mdpi.com/2076-3417/9/7/1488

[6] F. Seguel, N. Krommenacker, P. Charpentier, and I. Soto, "Visible light positioning based on architecture information: method and performance," *IET Communications*, vol. 13, no. 7, pp. 848–856, 2019. [Online]. Available: https://ietresearch.onlinelibrary.wiley.com/doi/abs/10.1049/iet-com.2018.5623

[7] Y. Almadani, D. Plets, S. Bastiaens, W. Joseph, M. Ijaz, Z. Ghassemlooy, and S. Rajbhandari, "Visible light communications for industrial applications—challenges and potentials," *Electronics*, vol. 9, no. 12, 2020. [Online]. Available: https://www.mdpi.com/2079-9292/9/12/2157

[8] Y. Almadani, M. Ijaz, W. Joseph, S. Bastiaens, S. Rajbhandari, B. Adebisi, and D. Plets, "A novel 3d visible light positioning method using received signal strength for industrial applications," *Electronics*, vol. 8, no. 11, 2019. [Online]. Available: https://www.mdpi.com/2079-9292/8/11/1311

[9] A. H. A. Bakar, T. Glass, H. Y. Tee, F. Alam, and M. Legg, "Accurate visible light positioning using multiple-photodiode receiver and machine learning," *IEEE Transactions on Instrumentation and Measurement*, vol. 70, pp. 1–12, 2021.

[10] Y.-C. Wu, C.-W. Chow, Y. Liu, Y.-S. Lin, C.-Y. Hong, D.-C. Lin, S.-H. Song, and C.-H. Yeh, "Received-signal-strength (rss) based 3d visible-light-positioning (vlp) system using kernel ridge regression machine learning algorithm with sigmoid function data preprocessing method," *IEEE Access*, vol. 8, pp. 214 269–214 281, 2020.

[11] F. Garbuglia, W. Raes, J. De Bruycker, N. Stevens, D. Deschrijver, and T. Dhaene, "Bayesian active learning for received signal strength-based visible light positioning," *IEEE Photonics Journal*, vol. 14, no. 6, pp. 1–8, 2022.

[12] Y. Chen, W. Guan, J. Li, and H. Song, "Indoor real-time 3-d visible light positioning system using fingerprinting and extreme learning machine," *IEEE Access*, vol. 8, pp. 13 875–13 886, 2020.

[13] K. Shailesh, "Energy efficient led lighting design for horticulture," in *2019 1st International Conference on Advanced Technologies in Intelligent Control, Environment, Computing and Communication Engineering (ICATIECE)*, 2019, pp. 339–342.

[14] Y. Almadani, M. Ijaz, W. Joseph, S. Bastiaens, S. Rajbhandari, B. Adebisi, and D. Plets, "A novel 3d visible light positioning method using received signal strength for industrial applications," *Electronics*, vol. 8, no. 11, 2019. [Online]. Available: https://www.mdpi.com/2079-9292/8/11/1311

[15] M. Ijaz, Z. Ghassemlooy, J. Pesek, O. Fiser, H. Le Minh, and E. Bentley, "Modeling of fog and smoke attenuation in free space optical communications link under controlled laboratory conditions," *Journal of Lightwave Technology*, vol. 31, no. 11, pp. 1720–1726, 2013.

[16] D. Plets, A. Eryildirim, S. Bastiaens, N. Stevens, L. Martens, and W. Joseph, "A performance comparison of different cost functions for rss-based visible light positioning under the presence of reflections," in *Proceedings of the 4th ACM Workshop on Visible Light Communication Systems*, ser. VLCS '17. New York, NY, USA: Association for Computing Machinery, 2017, p. 37–41. [Online]. Available: https://doi.org/10.1145/3129881.3129888

[17] S. Ma, J. Dai, S. Lu, H. Li, H. Zhang, C. Du, and S. Li, "Signal demodulation with machine learning methods for physical layer visible light communications: Prototype platform, open dataset, and algorithms," *IEEE Access*, vol. 7, pp. 30 588–30 598, 2019.

[18] B. Turan and S. Coleri, "Machine learning based channel modeling for vehicular visible light communication," *IEEE Transactions on Vehicular Technology*, vol. 70, no. 10, pp. 9659–9672, 2021.

[19] N. Knudde, W. Raes, J. De Bruycker, T. Dhaene, and N. Stevens, "Data-efficient gaussian process regression for accurate visible light positioning," *IEEE Communications Letters*, vol. 24, no. 8, pp. 1705–1709, 2020.